Graphical Abstract Rodriguez et al

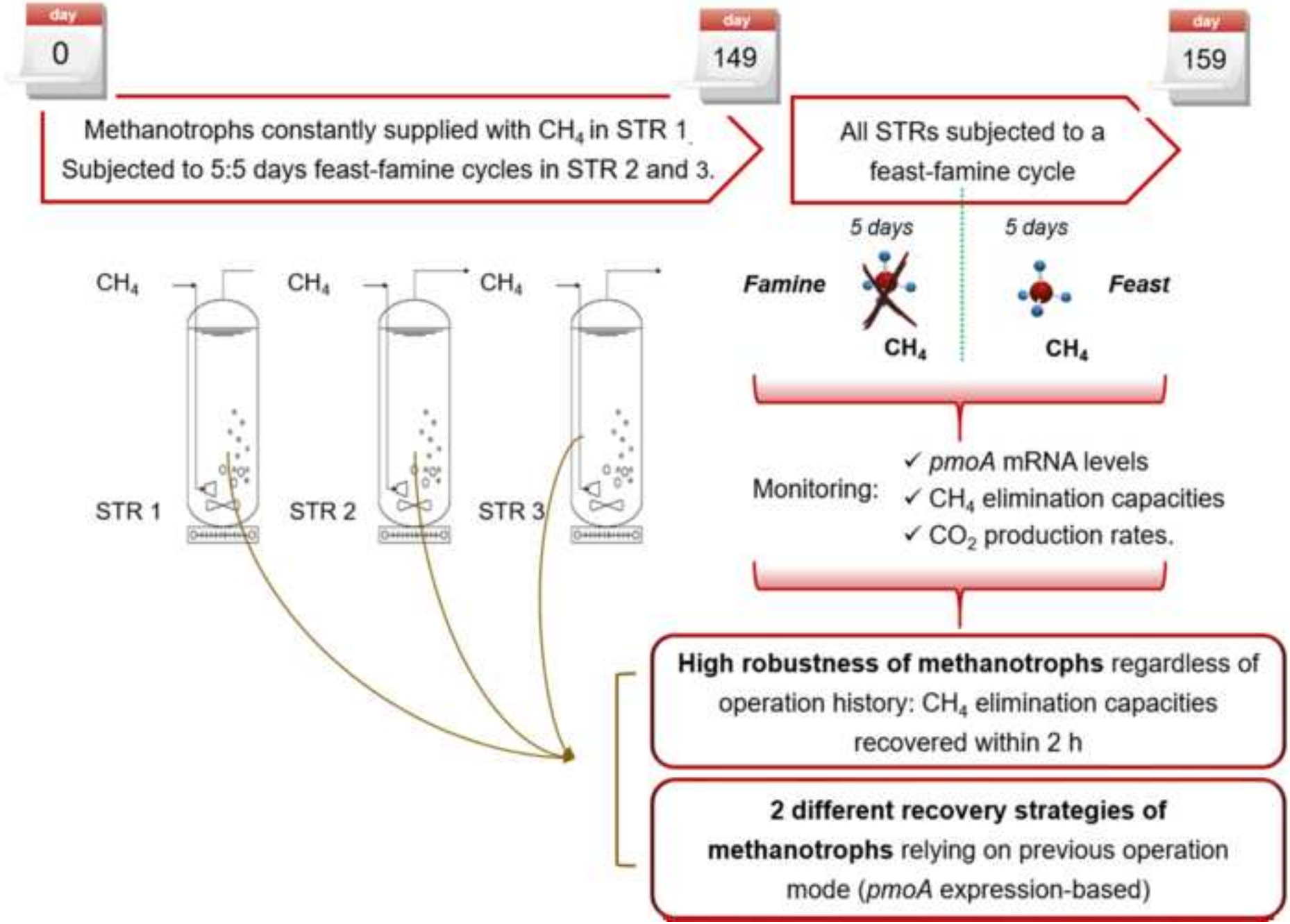

Highlights

- High robustness of CH_4-treatment biotechnologies towards inlet load fluctuations
- Recovery of CH_4 abatement performance within 1.5 – 2 h after CH_4 resumption
- Different recovery strategies (*pmoA*-based) of methanotrophs against CH_4 starvation

Quantitative analysis of methane monooxygenase (MMO) explains process robustness in continuous and feast-famine bioreactors treating methane

Elisa Rodríguez[a], Juan Carlos López[a], Patricia Prieto[a], Laura Merchán[a], Pedro A. García-Encina[a], Raquel Lebrero[a], Raúl Muñoz[a*]

[a] Department of Chemical Engineering and Environmental Technology. School of Industrial Engineering. University of Valladolid. Dr. Mergelina, s/n, 47011, Valladolid, Spain.

[*] Corresponding author: Department of Chemical Engineering and Environmental Technology. School of Industrial Engineering. University of Valladolid. Dr. Mergelina, s/n, 47011, Valladolid, Spain. Tel: +34-983-423166; E-mail: mutora@iq.uva.es

Abstract

The ability of methanotrophs to rapidly respond to intentional or accidental stress conditions caused by operational failures or process fluctuations is of utmost importance to guarantee the robustness of CH_4 abatement biotechnologies. In this study, the performance of a continuous and two feast-famine (5:5 days feast-famine cycles) stirred tank reactors treating diluted CH_4 emissions (4-5 % *v/v*) was comparatively assessed for 149 days. The robustness of the three bioreactors towards a 5 days CH_4 deprivation episode was thoroughly evaluated at a molecular level (*pmoA* gene expression level) and correlated to macroscopic process performance. The bioreactors recovered their steady-state abatement performance (in terms of CH_4 elimination capacity and CO_2 production rate) within 1.5 – 2 h following CH_4 supply resumption concomitantly with a maximum in *pmoA* gene expression, regardless of the previous operational mode. However, while methanotrophs from the continuous unit maintained higher basal levels of *pmoA* expression as a strategy for a rapid CH_4 metabolism initiation, the strategy of the feast-famine adapted-methanotrophs consisted on a more accurate regulation of their *pmoA* transcripts levels along with a higher and/or more rapid induction of the *pmoA* gene by CH_4 availability.

Keywords: expression level; gas treatment; load fluctuation; *pmoA*; robustness; transcripts

1 Introduction

Methane (CH_4), with a lifespan on Earth of ~12 years, is a short-lived greenhouse gas (GHG) (IPCC, 2014). This GHG possesses a global warming potential (GWP) 27 and 83 times higher than that of carbon dioxide (CO_2) in a 100-year and a 20-year horizon, respectively, and has been ranked the second most abundant GHG produced by anthropogenic activities after CO_2 (EEA, 2017; EPA, 2016; IPCC, 2014). Moreover, its actual global warming effect on Earth may be systematically underestimated since the United Nations and policymakers of the 100-year GWP use indistinctly the impact of both short-lived and long-lived GHGs as the default metric for its evaluation (Daniel et al., 2012; Ocko et al., 2017).

Today, flaring of CH_4-laden emissions is a common practice to safely dispose this potent GHG when present at concentrations > 30 % (*v/v*) (Nikiema et al., 2007). However, about 55 % of the anthropogenic CH_4 emissions contain CH_4 concentrations lower than 3 % (*v/v)*, which are not adequate for energy recovery purposes or for their treatment through conventional flaring (Avalos Ramirez et al., 2012; Nikiema et al., 2007). In this context, biotechnologies constitute a low-cost and sustainable alternative for CH_4 abatement at the low concentrations (<5 %) typically found in emissions from waste treatment activities, coal mining or animal farming (Scheutz et al., 2009).

To date, biofiltration constitutes the most studied and implemented biotechnology for CH_4 abatement, which can support high CH_4 removal efficiencies (RE) (> 90%) when parameters such as the O_2 concentration, moisture content and gas residence time are optimized (López et al., 2013). However, biomass accumulation in biofilters (typically entailing pressure drop increases, bed clogging and channeling problems) and their claimed poor robustness towards process fluctuations and failures, have limited the

widespread implementation of this technology (Cox and Deshusses, 1999; Devinny and Ramesh, 2005; Dorado et al., 2012). The application of starvation periods has been consistently proven as a simple and inexpensive way to control biomass accumulation in biofilters (Kim et al., 2005; Dorado et al., 2012; López et al., 2018), however, few data exist about the robustness of this strategy as compared to a continuous operation mode. Recently, the robustness (at macroscopic level) of biofilters operated under 3:3 and 5:5 days CH_4 feast-famine cycles (López et al., 2018) or subjected to a longer and single CH_4 famine period (30 days) has been assessed, observing a rapid recovery of the methanotrophic activity after the starvation conditions (Ferdowsi et al., 2016). In addition, studies in literature based on pure cultures of methanotrophs suggest that these bacteria possess regulatory mechanisms that allow them to survive well under starvation conditions (Roslev and King, 1994; Roslev and King, 1995). However, to demonstrate the robustness of this biomass control strategy compared to biofilter operation under continuous mode, dedicated studies at a molecular level (microbial robustness) correlated to a macroscopic process monitoring (CH_4 abatement) during feast-famine cycles are needed.

In this context, analyzing the response of methanotrophic bacteria through quantification of the expression of the key genes involved in CH_4 oxidation is a valuable but unexplored approach to understand process robustness towards sudden or cyclic fluctuations in the pollutant load. Quantification of the expression of the particulate methane monooxygenase gene (*pmoA*) (encoding the alpha subunit of the particulate methane monooxygenase (pMMO) enzyme catalyzing the conversion of CH_4 to methanol), is a widely used method to analyze methanotroph responses towards environmental fluctuations (McDonald et al., 2008). Besides copper and ammonia (NH_4^+), the concentration of the growth substrate (CH_4) regulates the expression of

pmoA gene and, consequently, methanotrophic activity (Baani and Liesack, 2008; Erikstad et al., 2012; Farhan Ul Haque et al., 2017). Tavormina and coworkers investigated the response of *pmoA* and other genes in a type II methanotroph (*Methyloprofundus sedimenti*) towards a short-term CH_4 starvation period followed by CH_4 supply resumption. Interestingly, *pmoA* expression declined in the presence of CH_4 and increased during CH_4 starvation as a strategy of *M. sedimenti* to be prepared to rapidly uptake CH_4 following substrate resumption (Tavormina et al., 2017).

In this study, the robustness (at the macroscopic and microscopic level) towards a feast-famine period (5:5 days CH_4 feast-famine cycles) of three stirred tank reactors (STRs) treating CH_4 at low concentrations (4-5 % *v/v*) was investigated. STR 1 was previously operated under continuous regime, while STR 2 and STR 3 were already acclimated to 5:5 days feast-famine cycles for 149 days. At day 149, a complete feast-famine cycle (5:5 days) was also applied to STR 1. From this day onwards, an intensive process monitoring of the macroscopic performance (based on CH_4 elimination capacities (ECs) and CO_2 production rates (PCO_2)), and of the transcriptional levels of the *pmoA* gene was conducted in the three STRs during the complete feast-famine cycle. This study aimed at elucidating the influence of the history of the microbial communities on their macroscopic and microscopic robustness towards the feast-famine periods typically encountered or intentionally applied in full-scale biofilters.

2 Material and methods

2.1 STRs configuration, inoculum and nutrient solution

The STRs consisted of cylindrical PVC columns (V = 3 L) top-sealed with butyl lids. A humidified air stream (93 ± 12 % of relative humidity) was mixed with a pure CH_4 stream (regulated with a mass flow controller, Aalborg USA) in a mixing chamber,

which resulted in a 4-5 % CH_4 air emission sparged at the bottom of the reactors using 2 µm metallic diffusers (Fig. 1). STR 2 and STR 3 were operated under feast-famine regimes, while STR 1 was operated under continuous mode. The STRs were inoculated with microbial consortia previously grown for 243 days in lab-scale biofilters (packed with K1 Kaldnes rings) treating CH_4 at low concentrations (4-5% *v/v*) under feast-famine (inocula of STR 2 and STR 3) or continuous mode (inoculum of STR 1) (López et al., 2018). The initial volatile suspended solid (VSS) concentration in STR 1, STR 2 and STR 3 was 8.8, 5.0 and 3.9 g L^{-1}, respectively. The cultivation broths were magnetically agitated at 800 rpm and maintained at 25 ± 1 °C during the entire experiment.

Centrate was used as a low-cost nutrient solution containing a high nutrients concentration and a low biodegradable organic fraction. This wastewater was obtained from the anaerobically digested sludge dewatering centrifuges of the Wastewater Treatment Plant (WWTP) of Valladolid and maintained at 4°C prior to use. Centrate was diluted with tap water at 1:2 ratio and supplemented with SO_4^{2-} at a final concentration of 150 mg L^{-1}. This diluted centrate was characterized by N-NH_4^+ concentrations of 170.84 ± 15.24 mg L^{-1}, pH values of 7.71 ± 0.12, inorganic carbon (IC) and total organic carbon (TOC) concentrations of 153.6 ± 11.4 mg L^{-1} and 12.82 ± 10.02 mg L^{-1}, respectively, and concentrations of P-PO_4^{3-}, N-NO_3^- and N-NO_2^- of 15.6 ± 3.4 mg L^{-1}, 2.2 ± 2.2 mg L^{-1} and 5.1 ± 3.4 mg L^{-1}, respectively. Liquid broth from the CH_4-supplemented STRs was retrieved and replaced by fresh diluted centrate at a rate of 225 mL d^{-1}. The biomass removed during the renewal of the nutrient solution was returned to the STRs after centrifugation (no biomass withdrawal) in order to mimic biofilter operating conditions.

2.2 STR operation and monitoring

The STRs were operated for 149 days before conducting the systematic evaluation of their robustness towards CH_4 deprivation. STR 1 was operated in a continuous mode, while STR 2 and STR 3 were operated under a feast-famine regime (5-days CH_4 starvation: 5-days CH_4 supply) in an alternate mode. The CH_4-laden air emission was continuously fed at 8 L h^{-1} to STR 1, and to STR 2 and STR 3 during their feast periods. During starvation conditions, the feast-famine units were supplied with a continuous CH_4-free air stream at 3 L h^{-1} to maintain the cultivation broth under aerobic conditions. The CH_4 inlet load (IL) in STR 1 and in STR 2 and STR 3 during the feast periods was 129.7 ± 6.2 g m^{-3} h^{-1}, which resulted in CH_4 concentrations of 48.0 ± 2.3 g m^{-3} (≈ 4-5 % v/v) and an empty bed residence time (EBRT) of 17.2 ± 0.0 min.

During the first 149 days of operation the performance was evaluated by monitoring the CH_4 and CO_2 gas concentrations at the inlet and outlet of the STRs during the feast periods at days 0, 1, 3 and 5 of each cycle and determining the CH_4 EC, PCO_2 and CO_2 production yield (YCO_2) as described in López et al. (2018). Additionally, 100 mL of cultivation broth from the STRs and the diluted centrate were used to determine once a week the concentration of NH_4^+, NO_3^-, NO_2^-, SO_4^{2-}, PO_4^{3-}, total suspended solids (TSS) and VSS. The pressure drop, temperature and pH of the cultivation broths were also periodically monitored.

2.3 Systematic evaluation of process robustness in continuous and feast-famine cultures

At day 149, STR 1 was operated under a feast-famine regime similar to STRs 2 and 3 in order to evaluate the macroscopic and microscopic response of the three bioreactors to starvation conditions, and the influence of the previous operation mode on *pmoA* expression and on the recovery of CH_4 oxidation activity following the resumption in

CH_4 supply. Thus, a complete 5:5 days feast-famine cycle was initiated at day 149, STR 1 and STR 2 being initially operated under famine conditions and STR 3 under feast conditions. The feast-famine cycle was thoroughly analyzed by sampling 10 mL of cultivation broth (for *pmoA* expression analysis by qPCR) at designated times: -1.7, 0.03, 0.25, 0.5, 1.0, 1.5, 2.0, 6.0, 12.0, 24.0, 72.0, 120.0 h during the first 5 days. Numbering was restarted for the second-half of the cycle so that sampling point t = 120.0 h of the first half of the cycle corresponded to sampling point t = -2.3 h for the second half of the cycle. Samples at 0.03, 0.25, 0.5, 1.0, 1.5, 2.0, 6.0, 12.0, 24.0, 72.0, 120.0 h were then collected during the second 5 days (feast period for STR 1 and STR 2; famine period for STR 3). CH_4 supply shutdown and resumption occurred at t = 0 h on each feast or famine half-cycle (Fig. 2). CH_4 and CO_2 gas concentrations at the inlet and outlet of the STRs were also determined at the above sampling times, except for the first 15 min after CH_4 supply shutdown and resumption (t = 0.25 h) to allow the renewal of the bioreactor headspace.

2.4 Analytical procedures

CH_4 and CO_2 gas concentrations in the gas phase and NH_4^+, NO_3^-, NO_2^-, SO_4^{2-} and PO_4^{3-} concentrations in the cultivation broth and centrate were determined according to López et al. (2018). The determination of TSS and VSS concentrations was performed according to standard methods (Eaton AD, Clesceri LS, Greenberg AE, 2005). Temperature and humidity of the inlet gas stream were on-line measured by a thermohygrometer (Testo 605-H1, Testo AG, Germany).

2.5 qPCR analyses

2.5.1 DNA and RNA isolation and cDNA generation

Cultivation broth samples for qPCR analyses were collected in sterile nuclease-free polypropylene tubes and immediately stored at -80 °C prior DNA/RNA extraction. DNA extraction was performed using the Fast® DNA Spin Kit for Soil (MP Biomedicals, LLC) according to the manufacturer but optimizing the time for cell lysis (130 s) in the Mini-Bead-beater equipment (Bio Spec Products, Inc.), and the time required (1 h) for optimal DNA binding to the silica matrix. DNA integrity was checked by agarose gel (1.2 % (*w/v*)) electrophoresis, while DNA concentrations were determined using a NanoDrop spectrophotometer (NanoDrop Technologies, Wilmington, USA).

Total RNA was purified using the RNeasy Plus Mini Kit (Qiagen Iberia SL) according to the manufacturer. Briefly, 900 µL (STR 1) and 1400 µL (STR 2 and STR 3) of cultivation broth sample were used for RNA extraction. After centrifugation, the pellet was resuspended in RLT buffer and then subjected to bead beating (2 min at 4800 rpm). Subsequently, a series of cleaning/purifying steps were carried out to recover the total RNA from samples. The total RNA obtained was subjected to a DNase treatment using the DNA-*free*™ DNA Removal Kit (ThermoFisher Scientific S.A.). DNase treatment reactions comprised 40 µl of purified RNA, 4 µl of DNase I Buffer and 1 µl of rDNase I. Digestion reactions were performed at 37 °C for 30 min and were subsequently inactivated by adding 4 µL of DNase Inactivation Reagent (2 min at room temperature). The DNase Inactivation Reagent was pelleted through centrifugation (5 min at 10000 rpm) allowing the DNA-free total RNA be recovered. The Experion™ RNA StdSens Analysis Kit (Bio-Rad Laboratories, Inc.) was used to assess the total RNA integrity in an Experion™ Automated Electrophoresis System (Bio-Rad Laboratories, Inc.). DNA-

free total RNA concentrations were quantified using a NanoDrop spectrophotometer (NanoDrop Technologies, Wilmington, USA). Then, the DNA-free total RNA was reverse transcribed to cDNA using the iScript™ Reverse Transcription Supermix for RT-qPCR (Bio-rad Laboratories, Inc.). The reactions were set up according to the manufacturer. The final concentration of DNA-free total RNA on each reaction was adjusted to 10 ng μL^{-1}. No-RT control reactions (no-reverse transcriptase) were also included to further detect the interference of genomic DNA contamination in RNA samples during the qPCR assays.

2.5.2 Generation of standard curves

Standard curves for the quantification of *pmoA* DNA and cDNA were constructed by cloning a 510 bp *pmoA* gene fragment (generated using the primer pair A189f/mb661r (Holmes et al., 1995; Costello and Lidstrom, 1999)) into the pCR4-TOPO plasmid vector (one-shot chemical transformation) using the TOPO TA cloning® kit for sequencing (Invitrogen, Carlsbad, CA). Clones bearing the target inserts were identified first by PCR screening using M13f and M13r-targeting vector sequences. Subsequently, positive clones were confirmed by sequencing using the above-mentioned primer pair, after plasmid DNA extraction with the Wizard® *Plus* SV Minipreps DNA Purification System (Promega, Madison, WI). Positive clones were stored at -80°C in 20 % (*v/v*) glycerol prior use for standard curve generation.

Plasmid DNA was isolated from a positive clone (deposited in GenBank under accession number MH025892) using the kit indicated above and then linearized by *spe*I restriction enzyme-based digestion (Promega, Madison, WI) at 37 °C for 4 h. The digestion mixture was prepared according to the manufacturer. The linearized plasmid was purified using the Wizard® DNA Clean-Up System (Promega, Madison, WI) and the resulting DNA plasmid concentration was measured using a NanoDrop

spectrophotometer (NanoDrop Technologies, Wilmington, USA). Plasmid DNA concentration (ng μL^{-1}) was transformed to copy number concentration of standard DNA molecules (copies μL^{-1}) using the following equation:

$$pmoA\left(\frac{\text{copy}}{\mu\text{L}}\right) = \frac{pmoA\ \text{concentration}\left(\frac{\text{ng}}{\mu\text{L}}\right)\times 6\times 10^{23}\left(\frac{\text{copy}}{\text{mol}}\right)}{\text{plasmid lenght (bp)}\times 6\times 10^{11}\left(\frac{\text{ng}}{\text{mol of bp}}\right)} \qquad \text{Eq. 1}$$

To avoid inter-run variation, a standard curve was run in triplicate on each qPCR assay (Fig. S1 and Fig. S2). Serial dilutions spanning 5 orders of magnitude (10^5 to 10^1 *pmoA* DNA or cDNA copies μL^{-1}) of the *pmoA* standard stock solution (3.9×10^5 copies μL^{-1}) were prepared to generate the standard curves. Serial dilutions used for quantification of cDNA from STR 3 spanned 4 orders of magnitude (10^5 to 10^2 *pmoA* cDNA copies μL^{-1}) (Fig. S1 and Fig. S2). The dilution series of standards were prepared once using large volume stock solutions, which were subsequently divided in 12 µL aliquots and maintained at -80°C prior to use, in order to reduce sampling errors during standard curve generation for each qPCR assay and enable calibration across a wider dynamic range (Svec et al., 2015).

2.5.3 qPCR and data treatment

qPCR of *pmoA* gene copies and gene transcripts was performed in a iCycler® Thermal Cycler coupled with an iQ5™ Multicolor Real-Time PCR detection system (Bio Rad Laboratories, Inc.). The aforementioned primer set A189f/mb661r was used to amplify a 510 bp fragment of the *pmoA* gene from the cultivation broth samples. PCR efficiency (*E*) and linearity (R^2) of each qPCR assay were determined using the slopes of the standards curves and using a linear regression analysis on the obtained data, respectively (Fig. S1 and Fig. S2). Primer specificity of the qPCR assay was optimized by applying a touchdown PCR program (Korbie and Mattick, 2008) (Table S1) and

adjusting the primer concentrations in the PCR reaction mixture. Primer specificity was confirmed by agarose gel electrophoresis (Fig. S3) and melting analysis (temperature range: 55°C - 95°C) (Fig. S4). PCR reactions were performed in 96-well reaction PCR plates. Each PCR reaction was set up to a final volume of 20 µL in each well containing 10 µL of SsoAdvanced™ Universal SYBR® Green Supermix (Bio-Rad Laboratories, Inc.), 1 µL of DNA or 2 µL of cDNA, 0.5 µL of each forward and reverse primers (250 nM final concentration) and nuclease-free water to complete the total reaction volume. Cycle threshold (Ct) values obtained for the standards and unknown samples were imported into Microsoft Excel for *pmoA* gene or transcript quantification. DNA standard curve concentrations were plotted as the linear regression of the Ct values of the amplification curves versus the log of the initial gene copy number. The concentration of the unknown samples (nº copies μL^{-1}) was determined by comparison of the Ct values of the target templates against the standard curve. The results obtained were converted to copy number per unit of volatile suspended solids (nº copy $mgVSS^{-1}$) to allow a fairer comparison of the STR microscopic performance. The relative expression level of the *pmoA* gene in each sample was calculated as the mRNA/DNA ratio (Yun et al., 2006; Freitag and Prosser, 2009), which indicates "per gene copy transcription level".

2.6 Statistical analysis

The software Statgraphics Centurion XV was used for the statistical analysis of the data. A parametric ANOVA Tukey test was conducted for the analysis of the STRs performance data before robustness assessment. Non-parametric procedures (Mann–Whitney Rank Sum and Kruskal–Wallis ANOVA) were carried out for the analysis of qPCR data during robustness analysis. Differences were considered significant at *P*-value ≤ 0.05.

3 Results and Discussion

3.1 Long-term performance of the STRs

Biomass concentrations of 4.0 ± 0.6, 1.8 ± 0.3 and 2.7 ± 0.5 g VSS L^{-1} were maintained in STR 1, STR 2 and STR 3, respectively during the long-term operation of the STRs. Despite the inoculation of the STRs with microorganisms acclimated to continuous and feast-famine feeding strategies, from 3 to 6 weeks were needed to reach a stable performance in terms of CH_4-EC in the STRs (Fig. 3). The performance of STR 1 was characterized by low and unstable ECs during approximately the first six weeks of operation (4.6 ± 1.3 g m^{-3} h^{-1} (~ 27 % EC variation)). Steady state CH_4-ECs of 12.8 ± 0.8 g m^{-3} h^{-1}) were recorded from day 47 onwards. Shorter initial instability periods were recorded in STR 2 (approx. 5 weeks) (10.0 ± 2.0 g m^{-3} h^{-1} (~ 20 % EC variation) and in STR 3 (approx. 3 weeks) (6.0 ± 0.7 g m^{-3} h^{-1} (~ 11 % EC variation). Steady state CH_4-ECs of 11.6 ± 0.8 g m^{-3} h^{-1} in STR 2 and 12.8 ± 0.8 g m^{-3} h^{-1} in STR 3 were recorded from day 35 and 20 onwards (Fig. 3). Despite similar ECs were recorded in the three STRs, a rigorous statistical analysis showed significant differences between STR 1 and STR 2 (p-value < 0.001) and between STR 2 and STR 3 (p-value = < 0.001), which revealed a slightly better performance of STRs 1 and 3. In this context, similar CH_4-ECs were reported for the three lab-scale biofilters used as inoculum in this study when operated under a 5-days / 5 days CH_4 feast-famine regime using almost identical IL and NH_4^+ concentration to those implemented in this study (López et al., 2018). Slightly lower CH_4 ECs (8 - 9 g m^{-3} h^{-1}) have been observed in a biofilter operated at similar ILs (95 g m^{-3} h^{-1}) and NH_4^+ concentrations (~0.15 g L^{-1}) at an EBRT of 4.3 min (Nikiema et al., 2009), while higher ECs (~45 g m^{-3} h^{-1}) were recorded in a biofilter supplied with an IL of 87 g m^{-3} h^{-1} but higher NH_4^+ concentrations (3 g L^{-1}) (EBRT of 6 min) (Ferdowsi et al., 2016). These results reflect the influence of nitrogen concentration on CH_4 EC.

For biofilters treating CH_4 ILs comprised between 55 and 95 g m^{-3} h^{-1}, an optimum nitrogen concentration (in the form of nitrate) of ~0.75 g L^{-1} has been previously observed (Nikiema et al., 2009).

PCO_2 of 11.6 ± 0.2 g m^{-3} h^{-1} were observed for the first 12 days of operation in STR 1, stabilizing afterwards at 25.0 ± 0.4 g m^{-3} h^{-1} (corresponding to a YCO_2 of 2.1 g CO_2 g CH_4^{-1}). PCO_2 in the feast-famine units reached steady values almost immediately, remaining at 21.5 ± 0.3 and 28.2 ± 0.4 g m^{-3} h^{-1} in STR 2 and STR 3, respectively, corresponding to YCO_2 values of 2.3 and 2.4 gCO_2 gCH_4^{-1} (Fig. 3). Statistically significant differences were found among all STRs (p-value = 0.0) in terms of PCO_2, STR 3 and STR 1 supporting slightly higher PCO_2 compared to STR 2, which was in accordance to their slightly superior CH_4 ECs. Comparable PCO_2 and YCO_2 values have been reported in literature in biofilters and biotrickling filters treating CH_4 under similar or higher CH_4 ILs (Estrada et al., 2014; Lebrero et al., 2015; López et al., 2018), which supports the hypothesis that higher ILs favor the use of CH_4 for maintenance rather than for methanotrophic biomass formation (Ferdowsi et al., 2016). In this context, the theoretical maximum mineralization yield of CH_4 accounts for 2.75 gCO_2 gCH_4^{-1}.

Steady state ammonium removal in the STRs was characterized by the accumulation of nitrate in the cultivation broth (74.1 ± 15.2, 94.5 ± 8.8, 98.3 ± 8.7 mg $N\text{-}NO_3^-$ L^{-1} in STR 1, STR 2 and STR 3, respectively), which suggested the development of a nitrifying consortia (detected through Illumina sequencing (data not shown)) and/or the contribution of methanotrophs to NH_4^+ oxidation. Negligible values of NO_2^- were detected in the cultivation broth of the STRs. STR 1 showed $N\text{-}NH_4^+$ REs (76.2 ± 5.8 %) significantly higher than the $N\text{-}NH_4^+$ REs in STR 2 (66.2 ± 4.2 %) (p-value = < 0.001) and STR 3 (66.6 ± 4.9 %) (p-value < 0.001). These $N\text{-}NH_4^+$ REs are higher than those observed in CH_4-abatement biofilters under similar NH_4^+ loading rates (Veillette

et al., 2011; López et al., 2018). On the other hand, the total nitrogen RE was also higher in STR 1 (31.1 ± 12.0 %) than in STR 2 (10.0 ± 8.4 %) and STR 3 (9.1 ± 8.0 %). These differences among the STRs in terms of N-NH_4^+ REs and total nitrogen RE were likely mediated by the higher biomass productivity of STR 1 induced by the continuous CH_4 supply. The different contribution of methanotrophs to NH_4^+ oxidation could have also played a key role on ammonia removal.

3.2 Assessment of process robustness in the continuous and feast/famine STRs

PCO_2 gradually decreased during starvation conditions following the sudden shutdown in CH_4 supply, reaching steady-state PCO_2 values of 5.9 ± 1.7 g m^{-3} h^{-1} (STR 1), 1.5 ± 0.5 g m^{-3} h^{-1} (STR 2) and 3.3 ± 1.6 g m^{-3} h^{-1} (STR 3) between hour 24 and 120 of the famine period as a result of the endogenous metabolism (Fig. 4). The unexpected increase in PCO_2 observed from the last sample of the previous feast period (t = -1.7 h) to the first sample of the famine period (t = 0.03 h) in the three units was likely due to the decrease in STR aeration from 8 to 3 L h^{-1}, which induced a pre-concentration of the residual CO_2 stripped out/generated from the cultivation broth during the first minutes of CH_4 deprivation (Fig. 4). Similar to PCO_2, *pmoA* mRNA/DNA ratios stabilized by the end of the famine cycle (from t = 24 - 72 h to t = 120 h), although in this case, a gradual decrease of the *pmoA* transcriptional activity was not observed during the first 12 hours of starvation (Fig. 5, Table 1). An initial decrease in the *pmoA* mRNA/DNA ratio (2 - 3-fold) was observed from t = -1.7 h to t = 0.03 h in the three STRs, followed by the recovery of the preceding ratio at t = 0.25 h in STR 1 or t = 0.5 h in STRs 2 and 3 (Fig. 5, Table 1). Subsequently, STR 1 was characterized by another decrease in the *pmoA* mRNA/DNA ratio by a factor of 5 at t = 0.5 h of starvation (compared to the preceding sample), followed by the recovery of the initial ratios (prior CH_4 supply shutdown) at 2 h of the famine cycle, and remaining constant during the following 10 h

(Fig. 5, Table 1). The *pmoA* mRNA/DNA ratios in STR 1 decreased to basal levels of expression at an average value of $1.7 \times 10^{-4} \pm 6.0 \times 10^{-5}$ from hour 24 to 120 (Fig. 5, Table 1). Interestingly, a pronounced decrease in the *pmoA* mRNA/DNA ratio was not observed in STR 2 and STR 3 during the first 12 h of starvation, which maintained their *pmoA* mRNA/DNA ratios almost constant or even slightly higher (STR 3). Hence, ~ 2-fold variations in the *pmoA* gene expression level were recorded in STR 2 (Fig. 5, Table 1) until basal expression levels ($4.7 \times 10^{-6} \pm 1.6 \times 10^{-6}$) were reached from t = 24 h to t = 120 h (Table 1). STR 3 showed a slight increase in the *pmoA* transcriptional activity (3× higher compared to t = -1.7 h), which initiated at t = 0.25 h and peaked at t = 1.5 h. Then, the *pmoA* gene expression decreased to basal levels (average ratio of $2.6 \times 10^{-6} \pm 8.2 \times 10^{-7}$) from t = 72 h onwards. Overall, the variations in the *pmoA* mRNA/DNA ratio in the three STRs during the first 12 hours of starvation suggest an early *pmoA* regulation in response to the sudden CH_4 shutdown until steady-state *pmoA* mRNA/DNA levels were reached.

Similar CH_4-ECs to those observed prior CH_4 supply shutdown (16.3, 16.8 and 16.1 g m^{-3} h^{-1} in STR 1, 2 and 3, respectively) were achieved within the first 1 - 2 h following CH_4 supply resumption (Fig. 6). Similarly, PCO_2 comparable to those recorded under steady state in the previous CH_4 feast period were reached within the first 2 hours following CH_4 supply restoration in the three STRs (Fig. 4). A transient induction of the gene (sharp increase in the *pmoA* mRNA/DNA ratio) mediated by the enhanced CH_4 availability was observed during the first 12 h - 24 h of the feast cycle in the three STRs (Fig. 5, Table 1). Then, the *pmoA* mRNA/DNA ratios stabilized at basal levels of expression (Fig. 5, Table 1). This expression pattern characterized by a pronounced increase in the *pmoA* transcriptional activity at the initial stage of recovery, followed by

a return to basal levels of expression, is typical of stress-induced genes. In fact, the gene expression response (induction or repression) after a transient or persistent exposure to stressors finally returns to steady-state levels close to those present in unstressed cells (Fong et al., 2005; López-Maury et al., 2008). Maximum *pmoA* mRNA/DNA ratios during transient *pmoA* induction were recorded at 2 h, 1.5 h and 2 - 6 h after CH_4 supply restoration in STR 1, STR 2 and STR 3, respectively (Fig. 5, Table 1). The periods matched with the time needed to recover steady state CH_4-ECs (1.5 - 2 h following CH_4 supply resumption) (Fig. 6). This suggests a rapid physiological adaptation of methanotrophs to the new environmental conditions and explains the quick recovery of the CH_4-EC in the three STRs within less than 2 h, thus revealing an outstanding process robustness regardless of the previous operation mode. Similar results in terms of CH_4-EC were observed by López et al. (2018) in biofilters operated under 5:5 days feast-famine cycles at similar CH_4 ILs. Lebrero et al. (2010) also observed a fast recovery (30 min) of the previous ECs of butanone, toluene and H_2S (fed at trace level concentrations (mg m^{-3})) in biofilters and air diffusion bioreactors subjected to 3-day pollutant starvation periods. In contrast, 5 days were needed to reach the previous process performance in a biofilter operated at an IL of 13 g m^{-3} h^{-1} after a 30-day CH_4 and nutrients starvation period (Ferdowsi et al., 2016). At this point it should be highlighted that our study constitutes, to the best of our knowledge, the first evaluation of *pmoA* gene expression (key functional gene involved in CH_4 oxidation) in CH_4-treating bioreactors.

The apparently high CH_4-ECs (45-66 g m^{-3} h^{-1}) recorded immediately after CH_4 supply restoration (maximum CH_4-EC at t = 0.03 h in STR 1 and 2 and at t = 0.5 h in STR 3) in all bioreactors were likely mediated by the high headspace volumes of the STR compared to the CH_4-laden emission rates (Fig. 6). Therefore, these initial CH_4-ECs

probably do not represent the real ECs at the gas-liquid interphase of the reactors, since the CH_4 concentrations measured at the outlet gas sampling ports were diluted with the CH_4 free air initially present at the headspace of the STRs. In fact, these high CH_4-ECs occurred before induction of the *pmoA* gene, which would entail similar or even lower CH_4 oxidation activities if a direct correlation between CH_4 oxidation and *pmoA* mRNA/DNA ratio is assumed. This rules out the potential biological basis of the large CH_4-ECs recorded during this period. Similarly, the high CO_2 concentrations recorded during the first 30 min following CH_4 restoration in STR 2 and STR 3 (Fig. 4) were probably not induced by higher CH_4 oxidation activities but by the enhanced stripping (caused by the higher aeration rates) of CO_2 generated by non-methanotrophic methylotrophs or denitrifying bacteria (detected in this study through Illumina sequencing (data not shown)) (Nikiema et al., 2009).

3.3 Different survival strategies of methanotrophs explain process robustness in continuous and feast-famine STRs

The monitoring of the *pmoA* mRNA/DNA ratio revealed common and differential aspects in the regulation of *pmoA* gene expression between methanotrophs non-adapted and adapted to cyclic fluctuations in CH_4 supply (continuous *vs* feast-famine operation). Interestingly, the trend observed in the expression of the *pmoA* gene in the methanotrophs from the feast-famine units suggests an adaptation of the *pmoA* gene expression program to the long-term cyclic stress conditions (feast-famine) imposed. The basal levels of *pmoA* expression during feast and famine conditions (t = 24 h to t = 120 h) in STRs 2 and 3 were significantly lower (two orders of magnitude under famine regime, one order of magnitude during feast regime) than those observed in STR 1 (p-value < 0.001) (Table 1). This lower expression levels of the *pmoA* gene in the feast-famine units could represent a beneficial evolutionary adaptation acquired due to the

repeated famine stress, since stress conditions not only promote short-term adaptations but may act as a major driving force for evolutionary innovation (López-Maury et al., 2008). Some authors have hypothesized that the conserved intracellular ATP that would result from a reduced expression of these genes potentially represents a factor driving faster adaptation of bacteria to stress (Fong et al., 2005).

On the other hand, the differences in basal levels of *pmoA* transcription between feast and famine conditions were higher in STR 2 and STR 3 (adapted to feast-famine operation) than in STR1 (adapted to continuous operation), which maintained similar *pmoA* basal expression levels during the feast and starvation periods (Fig. 5, Table 1). The maintenance of high levels of *pmoA* expression during starvation (even higher than those observed under CH_4 supply) have been observed in bacteria typically inhabiting oligotrophic environments where longer periods of starvation can occur. This has been considered as a survival strategy that facilitate the resumption of microbial growth immediately upon substrate replenishment (Bollmann et al., 2005; Tavormina et al., 2017). On the contrary, methanotrophs in STR 2 and STR 3 seem to have adopted a different recovery strategy through fine-tuning of *pmoA* gene expression regulation acquired due to the repeated exposure to feast-famine cycles. In fact, in addition to the above-mentioned lower basal levels of expression, the regulation of *pmoA* in methanotrophs from STR 2 and STR 3 was characterized by a decrease in the *pmoA* mRNA/DNA ratio from the last sample of the famine period (t = 120 h) to the first sample of the feast period (t = 0.03 h). However, *pmoA* expression rapidly recovered fifteen minutes later (t = 0.25 h) (Table 1). It seems that the *de novo* synthesis of *pmoA* transcripts decelerated immediately after the resumption of CH_4 supply in order to maximize ATP conservation until CH_4 was effectively available in the cultivation broth. Interestingly, the intensity of the induction of the *pmoA* gene during the first 12 -24 h of

the feast period was higher in STRs 2 and 3. Thus, based on the lowest *pmoA* mRNA/DNA ratio at the end of the famine cycle (t =120 h for STR 1) or immediately after the resumption of CH_4 supply (t = 0.03 h for STRs 2 and 3), the maximum *pmoA* mRNA/DNA ratio recorded during the feast period increased over one order of magnitude in STR 1 (from 1.3×10^{-4} to 1.6×10^{-3}), two orders of magnitude in STR 3 (from 6.9×10^{-7} to 5.3×10^{-5}) and four orders of magnitude in STR 2 (from 4.4×10^{-7} to 2.1×10^{-3}) (Table 1). These results are consistent with the hypothesis of a transcriptional adaptation or transcriptional memory acquired along the cyclic stress events (feast-famine), which has been consistently observed by other authors (López-Maury et al., 2008 ; Lambert and Kussel, 2014).

Altogether, these results revealed two different recovery strategies of methanotrophic activity in response to CH_4 starvation as a function of the previous operational mode (continuous *vs* feast-famine). The methanotrophic communities present in the continuous and feast-famine units exhibited a response memory: a behavior in which gene expression persists after removal of an external inducer (Lambert and Kussel, 2014). However, methanotrophs in STR 1 based their recovery strategy on the maintenance of higher basal levels of *pmoA* expression as a strategy to quickly oxidize CH_4 upon replenishment. This strategy has been typically observed in bacteria adapted to changing environments where unexpected fluctuations can occur (Bollmann et al., 2005; Tavormina et al., 2017). However, this survival strategy did not seem to be optimal in the case of environments where an expected programmed fluctuation (i.e. feast-famine cycle) prevail, due to the high energy costs associated to an unnecessary *pmoA* transcription during the famine period. In STR 2 and STR 3, methanotrophs avoided such long-term energy cost by finely regulating the quantity of *pmoA* transcripts necessary for CH_4 oxidation activity, which likely entailed maximal

metabolic costs through transient induction of the *pmoA* gene during the first hours following the restoration of CH_4 supply (Fig. 5). This metabolic cost is typically determined by the duration of this transient expression (Lambert and Kussel, 2014) and likely, by the intensity of the induction. In this study, STR 2 exhibited a stronger but shorter induction compared to STR 3, although both units experienced a higher induction than STR 1 during the recovery of CH_4 oxidation (Fig. 5, Table 1). These results suggest an adaptation of methanotrophs to a cyclic fluctuating environment (feast-famine) by adjusting *pmoA* gene expression levels, and confirm that gene expression levels may be evolutionarily tuned not only to support growth in a single environment, but also to provide cells' progeny with memory of past environments (Lambert and Kussel, 2014).

4 Conclusions

This study demonstrated at a macroscopical and molecular level the robustness of CH_4-treatment biotechnologies towards sudden or cyclic fluctuations in pollutant load regardless of the previous operational mode (continuous in STR 1, feast-famine in STRs 2 and 3). The steady-state CH_4 biodegradation performance was recovered within the first 1.5 – 2 h after CH_4 resumption concomitantly with a maximum in *pmoA* gene expression, which suggested a rapid response of methanotrophs to CH_4 availability. Although a comparable recovery capacity was recorded in the three STRs, two different strategies against CH_4 deprivation were observed as a result of the previous operational mode. Thus, methanotrophs in STR 1 maintained high basal levels of *pmoA* expression as a strategy to be set to rapidly oxidize CH_4 upon replenishment. On the contrary, methanotrophs in STR 2 and STR 3 reduced their basal levels of expression of the *pmoA* gene and finely regulated the quantity of *pmoA* transcripts necessary to support CH_4 oxidation activity. Unfortunately, whether these two different recovery strategies

impacted or not on the maximum CH_4 biodegradation capacity of the methanotrophs fed continuously or under a feast-famine regime was impossible to elucidate in this work due to ultimate occurrence of CH_4 mass transfer limitations (similarly to the scenario encountered in biofilters or biotrickling filters). Overall, this work consistently demonstrated the outstanding robustness of methanotrophs, whose metabolism was not significantly damaged under 5-days starvation periods and fully recovered within 1.5 – 2 h after CH_4 supply resumption.

Acknowledgements

This research was funded by the Spanish Ministry of Economy and Competitiveness and the European Union through the FEDER Funding Program (CTM2015-70442-R and Red Novedar) and Juan de la Cierva Program (18I.SMW). The financial support from the Regional Government of Castilla y León is also gratefully acknowledged (UIC71). The authors wish to thank Alejandra Martínez for help in sequence analysis and submission.

Declarations of interest:

None

References

Avalos Ramirez, A., Jones, J.P., Heitz, M., 2012. Methane treatment in biotrickling filters packed with inert materials in presence of a non-ionic surfactant. J. Chem. Technol. Biotechnol. 87, 848–853. doi:10.1002/jctb.3811

Baani, M., Liesack, W., 2008. Two isozymes of particulate methane monooxygenase with different methane oxidation kinetics are found in *Methylocystis* sp. strain SC2. Proc. Natl. Acad. Sci. U. S. A. 105, 10203–10208. doi:10.1073/pnas.0702643105

Bollmann, A., Schmidt, I., Saunders, A.M., Nicolaisen, M.H., 2005. Influence of starvation on potential ammonia-oxidizing actvity and *amoA* mRNA levels in *Nitrospira briensis*. Appl. Environ. Microbiol. 71, 1276–1282. doi:10.1128/AEM.71.3.1276-1282.2005

Costello, A.M., Lidstrom, M.E., 1999. Molecular characterization of functional and phylogenetic genes from natural populations of methanotrophs in lake sediments. Appl Env. Microbiol 65, 5066–5074.

Cox, H.H.J., Deshusses, M.A., 1999. Biomass control in waste air biotrickling filters by protozoan predation. Biotechnol. Bioeng. 62, 216–224. doi:10.1002/(SICI)1097-0290(19990120)62:2<216::AID-BIT12>3.0.CO;2-4

Daniel, J.S., Solomon, S., Sanford, T.J., McFarland, M., Fuglestvedt, J.S., Friedlingstein, P., 2012. Limitations of single-basket trading: lessons from the Montreal Protocol for climate policy. Clim. Change 111, 241–248. doi:10.1007/s10584-011-0136-3

Devinny, J.S., Ramesh, J., 2005. A phenomenological review of biofilter models. Chem. Eng. J. 113, 187–196. doi:10.1016/j.cej.2005.03.005

Dorado, A.D., Baeza, J.A., Lafuente, J., Gabriel, D., Gamisans, X., 2012. Biomass accumulation in a biofilter treating toluene at high loads - Part 1: Experimental performance from inoculation to clogging. Chem. Eng. J. 209, 661–669. doi:10.1016/j.cej.2012.08.018

Eaton, A.D., Clesceri, L.S., Greenberg, A.E., Franson, M.A.H., 2005. Standard methods for the examination of water and wastewater. American Public Health Association, Washington DC.

EEA, 2017. Annual European Union greenhouse gas inventory 1990 - 2015 and inventory report 2017. European Environment Agency.

EPA, 2016. Inventory of U.S. greenhouse gas emissions and sinks: 1990 - 2016. United States Environmental Protection Agency.

Erikstad, H.A., Jensen, S., Keen, T.J., Birkeland, N.K., 2012. Differential expression of particulate methane monooxygenase genes in the verrucomicrobial methanotroph "*Methylacidiphilum kamchatkense*" Kam1. Extremophiles 16, 405–409. doi:10.1007/s00792-012-0439-y

Estrada, J.M., Lebrero, R., Quijano, G., Pérez, R., Figueroa-González, I., García-Encina, P.A., Muñoz, R., 2014. Methane abatement in a gas-recycling biotrickling filter: Evaluating innovative operational strategies to overcome mass transfer limitations. Chem. Eng. J. 253, 385–393. doi:10.1016/j.cej.2014.05.053

Farhan Ul Haque, M., Gu, W., Baral, B.S., DiSpirito, A.A., Semrau, J.D., 2017. Carbon source regulation of gene expression in *Methylosinus trichosporium* OB3b. Appl. Microbiol. Biotechnol. 101, 3871–3879. doi:10.1007/s00253-017-8121-z

Ferdowsi, M., Veillette, M., Ramirez, A.A., Jones, J.P., Heitz, M., 2016. Performance

Evaluation of a Methane Biofilter Under Steady State, Transient State and Starvation Conditions. Water. Air. Soil Pollut. 227, 168. doi:10.1007/s11270-016-2838-7

Fong, S.S., Joyce, A.R., Palsson, B.Ø., 2005. Parallel adaptive evolution cultures of *Escherichia coli* lead to convergent growth phenotypes with different gene expression states. Genome Res. 15, 1365–1372. doi:10.1101/gr.3832305

Freitag, T.E., Prosser, J.I., 2009. Correlation of methane production and functional gene transcriptional activity in a peat soil. Appl. Environ. Microbiol. 75, 6679–6687. doi:10.1128/AEM.01021-09

Holmes, A.J., Costello, A., Lidstrom, M.E., Murrell, J.C., 1995. Evidence that particulate methane monooxygenase and ammonia monooxygenase may be evolutionary related. FEMS Microbiol.Lett. 132, 203–208.

IPCC, 2014. Climate change 2014 Synthesis Report. Contribution of Working Groups I, II and III to the Fifth Assessment Report of the Intergovernmental Panel on Climate Change. doi:10.1017/CBO9781107415324

Kim, D., Cai, Z., Sorial, G.A., 2005. Behavior of trickle-bed air biofilter for toluene removal: Effect of non-use periods. Environ. Prog. 24, 155–161. doi:10.1002/ep.10079

Korbie, D.J., Mattick, J.S., 2008. Touchdown PCR for increased specificity and sensitivity in PCR amplification. Nat. Protoc. 3, 1452–1456. doi:10.1038/nprot.2008.133

Lambert, G., Kussel, E., 2014. Memory and Fitness Optimization of Bacteria under Fluctuating Environments. PLoS Genet. 10, e1004556.

doi:10.1371/journal.pgen.1004556

Lebrero, R., Hernández, L., Pérez, R., Estrada, J.M., Muñoz, R., 2015. Two-liquid phase partitioning biotrickling filters for methane abatement: Exploring the potential of hydrophobic methanotrophs. J. Environ. Manage. 151, 124–131. doi:10.1016/j.jenvman.2014.12.016

Lebrero, R., Rodríguez, E., Martin, M., García-Encina, P.A., Muñoz, R., 2010. H_2S and VOCs abatement robustness in biofilters and air diffusion bioreactors: A comparative study. Water Res. 44, 3905–3914. doi:10.1016/j.watres.2010.05.008

López-Maury, L., Marguerat, S., Bähler, J., 2008. Tuning gene expression to changing environments: from rapid responses to evolutionary adaptation. Nat. Rev. Genet. 9, 583–593. doi: 10.1038/nrg2398

López, J.C., Merchán, L., Lebrero, R., Muñoz, R., 2018. Feast-famine biofilter operation for methane mitigation. J. Clean. Prod. 170, 108–118. doi:10.1016/j.jclepro.2017.09.157

López, J.C., Quijano, G., Souza, T.S.O., Estrada, J.M., Lebrero, R., Muñoz, R., 2013. Biotechnologies for greenhouse gases (CH_4, N_2O, and CO_2) abatement: State of the art and challenges. Appl. Microbiol. Biotechnol. 97, 2277–2303. doi:10.1007/s00253-013-4734-z

McDonald, I.R., Bodrossy, L., Chen, Y., Murrell, J.C., 2008. Molecular ecology techniques for the study of aerobic methanotrophs. Appl. Environ. Microbiol. 74, 1305–1315. doi:10.1128/AEM.02233-07

Nikiema, J., Brzezinski, R., Heitz, M., 2007. Elimination of methane generated from landfills by biofiltration: a review. Rev. Environ. Sci. Bio/Technology 6, 261–284.

doi:10.1007/s11157-006-9114-z

Nikiema, J., Girard, M., Brzezinski, R., Heitz, M., 2009. Biofiltration of methane using an inorganic filter bed: Influence of inlet load and nitrogen concentration. Can. J. Civ. Eng. 36, 1903–1910. doi:10.1139/L09-144

Ocko, I.B., Hamburg, S.P., Jacob, D.J., Keith, D.W., Keohane, N.O., Oppenheimer, M., Roy-Mayhew, J., Schrag, D.P., Pacala, S.W., 2017. Unmask temporal trade-offs in climate policy debates. Science 356, 492–493. doi: 10.1126/science.aaj2350

Roslev, P., King, G.M., 1995. Aerobic and anaerobic starvation metabolism in methanotrophic bacteria. Appl. Environ. Microbiol. 61, 1563–1570.

Roslev, P., King, G.M., 1994. Survival and recovery of methanotrophic bacteria starved under oxic and anoxic conditions. Appl. Environ. Microbiol. 60, 2602–2608.

Scheutz, C., Kjeldsen, P., Bogner, J.E., De Visscher, A., Gebert, J., Hilger, H.A., Huber-Humer, M., Spokas, K., 2009. Microbial methane oxidation processes and technologies for mitigation of landfill gas emissions. Waste Manag. Res. 27, 409–455. doi:10.1177/0734242X09339325

Svec, D., Tichopad, A., Novosadova, V., Pfaffl, M.W., Kubista, M., 2015. How good is a PCR efficiency estimate: Recommendations for precise and robust qPCR efficiency assessments. Biomol. Detect. Quantif. 3, 9–16. doi:10.1016/j.bdq.2015.01.005

Tavormina, P.L., Kellermann, M.Y., Antony, C.P., Tocheva, E.I., Dalleska, N.F., Jensen, A.J., Valentine, D.L., Hinrichs, K.U., Jensen, G.J., Dubilier, N., Orphan, V.J., 2017. Starvation and recovery in the deep-sea methanotroph *Methyloprofundus sedimenti*. Mol. Microbiol. 103, 242–252.

doi:10.1111/mmi.13553

Veillette, M., Viens, P., Ramirez, A.A., Brzezinski, R., Heitz, M., 2011. Effect of ammonium concentration on microbial population and performance of a biofilter treating air polluted with methane. Chem. Eng. J. 171, 1114–1123. doi:10.1016/j.cej.2011.05.008

Yun, J.J., Heisler, L.E., Hwang, I.I.L., Wilkins, O., Lau, S.K., Hyrcza, M., Jayabalasingham, B., Jin, J., McLaurin, J.A., Tsao, M.S., Der, S.D., 2006. Genomic DNA functions as a universal external standard in quantitative real-time PCR. Nucleic Acids Res. 34, e85. doi:10.1093/nar/gkl400

Figure Captions

Figure 1. Experimental set-up. 1 Methane cylinder, 2 Mass flow controller, 3 Mixing chamber, 4 Humidifying column, 5 Compressor, 6 Ambient air, 7 Gas outlet, 8 Rotameter. STR 1 Stirred tank reactor, STR 2 and STR 3 Feast-famine stirred tank reactors.

Figure 2. Schematic overview of the sampling collection times during a complete feast-famine cycle for *pmoA* transcription analysis by qPCR. a) Samples collected during the first 5 days of the feast-famine cycle (famine for STR 1 and STR 2; feast for STR 3). b) Samples collected during the second 5 days of the feast-famine cycle (feast for STR 1 and STR 2; famine for STR 3). Samples for the determination of gas concentration were collected simultaneously except for samples corresponding to 15 min following shutdown or resumption of CH_4 supply (t = 0.25 h), which were only collected for qPCR analysis.

Figure 3. Time course of the IL (black dotted line), EC (dark blue triangle) and PCO_2 (green square) in STR 1 (a), STR 2 (b) and STR 3 (c) during long-term performance.

Figure 4. Time course of PCO_2 during the 5:5 days feast-famine cycle in STR 1 (dark blue continuous line), STR 2 (pink dashed line) and STR 3 (green dotted line). The vertical dashed black lines indicate CH_4 supply shutdown and resumption. Reduced-size upper graphs show the detail of PCO_2 dynamics during the first 12 h of famine (left) or feast (right) conditions for the three STRs.

Figure 5. a) Time course of the *pmoA* mRNA/DNA ratio during the 5:5 days feast-famine cycle in STR 1 (dark blue continuous line), STR 2 (pink dashed line) and STR 3 (green dotted line). Reduced-size upper graphs show the detail of *pmoA* mRNA/DNA

ratio variations during the first 12 h of famine (left) or feast (right) conditions for the three STRs. Some sampling points are indicated on the graph for clarity purposes. b) Detail of *pmoA* mRNA/DNA ratio dynamics during the first 12 h of famine (left) or feast (right) conditions for STR 1 (dark blue continuous line), STR 2 (pink dashed line) and STR 3 (green dotted line). One graph per STR under feast or famine condition is presented using different numeric scale in order to appreciate *pmoA* mRNA/DNA ratio variations. The vertical dashed black lines indicate CH_4 supply shutdown and resumption.

Figure 6. Time course of the EC during the 5:5 days feast-famine cycle in STR 1 (dark blue continuous line), STR 2 (pink dashed line) and STR 3 (green dotted line). The vertical dashed black lines indicate CH_4 supply shutdown and resumption. Reduced-size upper graphs show the detail of CH_4 EC dynamics during the first 12 h of famine (left) or feast (right) conditions for the three STRs.

Figure 1.

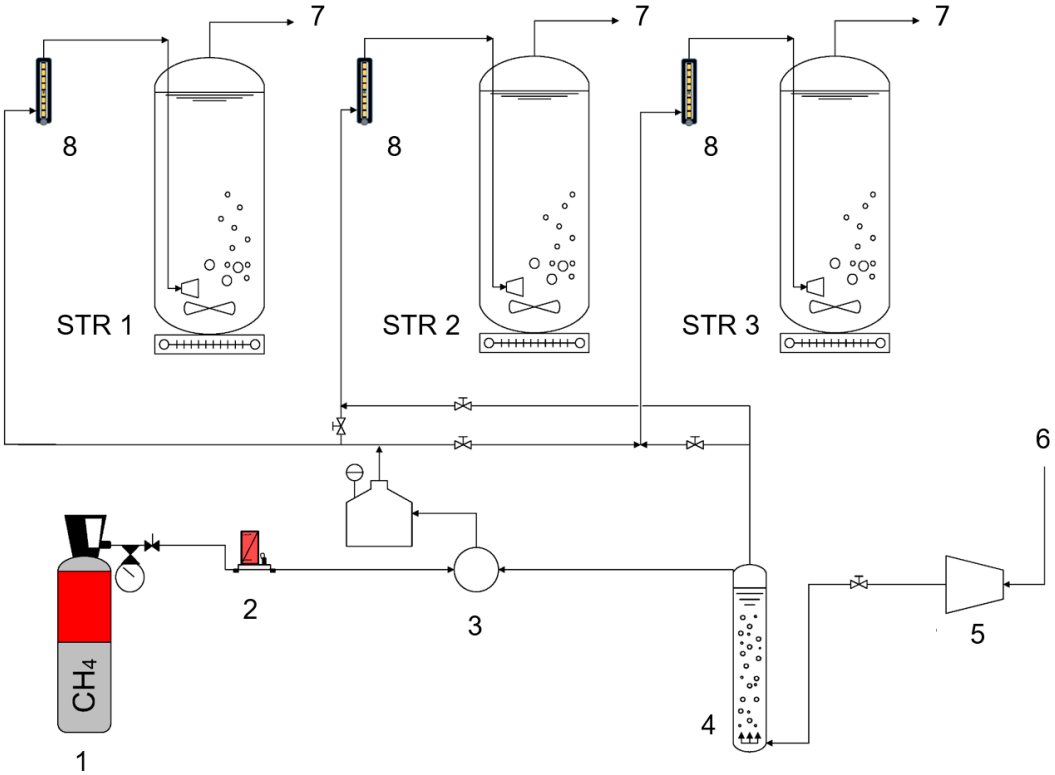

Figure 2.

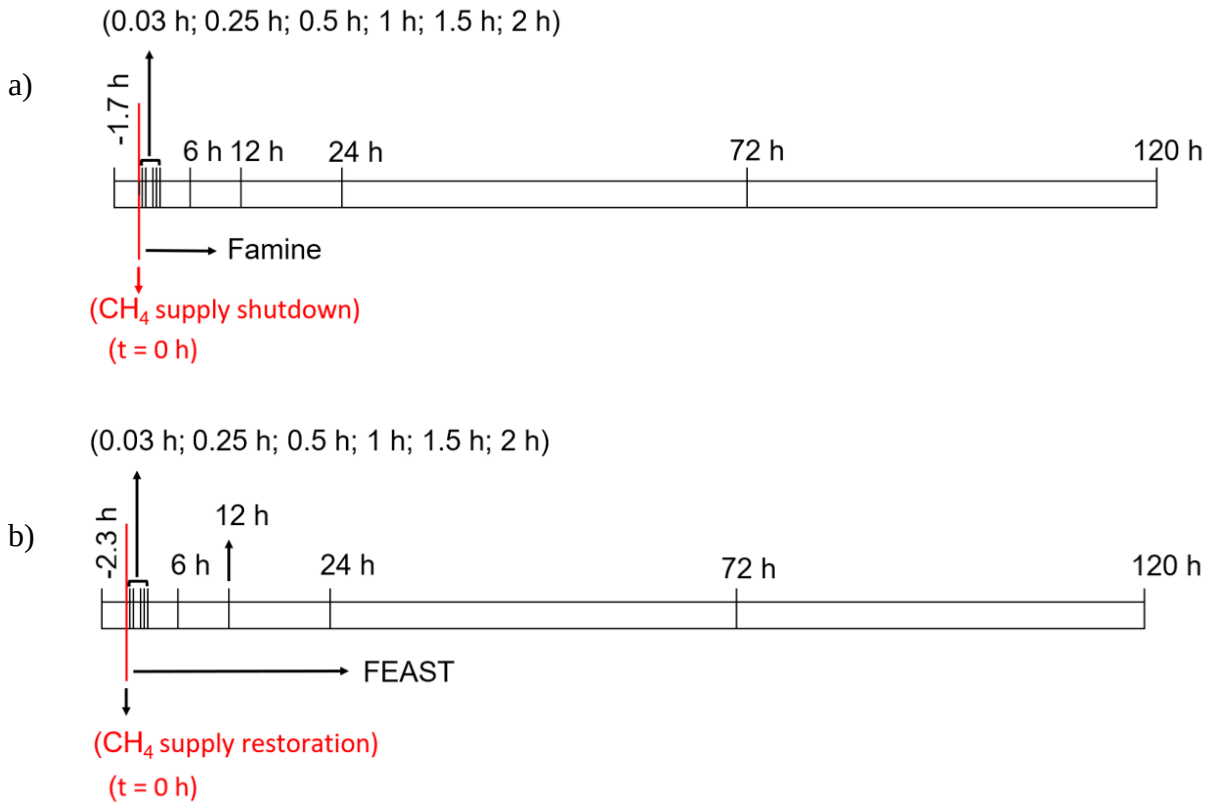
a)
(0.03 h; 0.25 h; 0.5 h; 1 h; 1.5 h; 2 h)
-1.7 h
6 h
12 h
24 h
72 h
120 h
Famine
(CH4 supply shutdown)
(t = 0 h)
b)
(0.03 h; 0.25 h; 0.5 h; 1 h; 1.5 h; 2 h)
-2.3 h
12 h
6 h
24 h
72 h
120 h
FEAST
(CH4 supply restoration)
(t = 0 h)

Figure 3.

a)

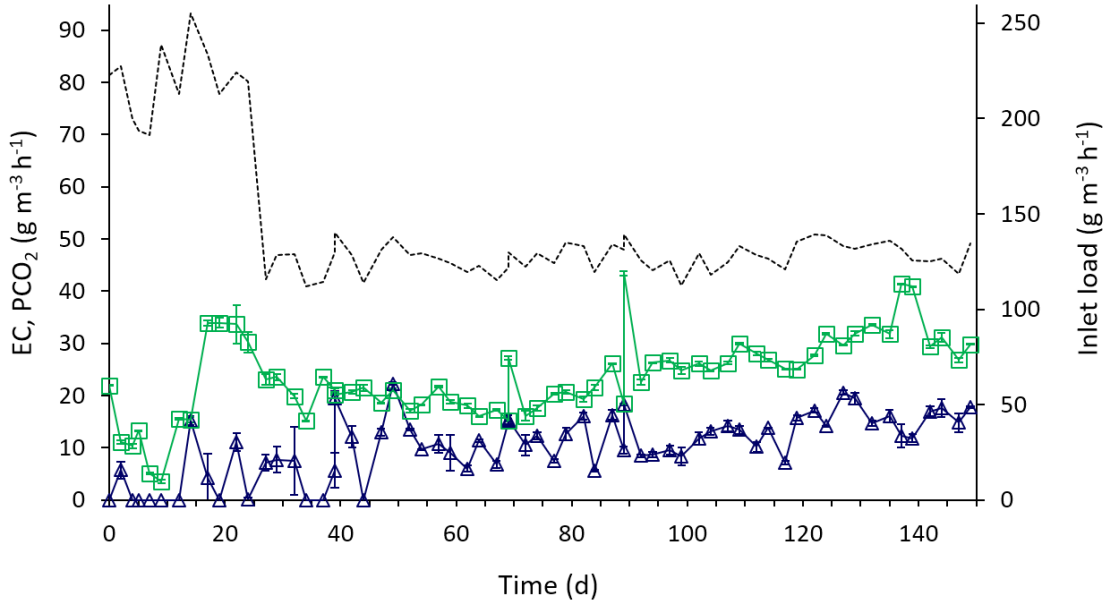
EC, PCO2 (g m-3 h-1)
Inlet load (g m-3 h-1)
Time (d)
0
10
20
30
40
50
60
70
80
90
0
50
100
150
200
250
0
20
40
60
80
100
120
140

b)

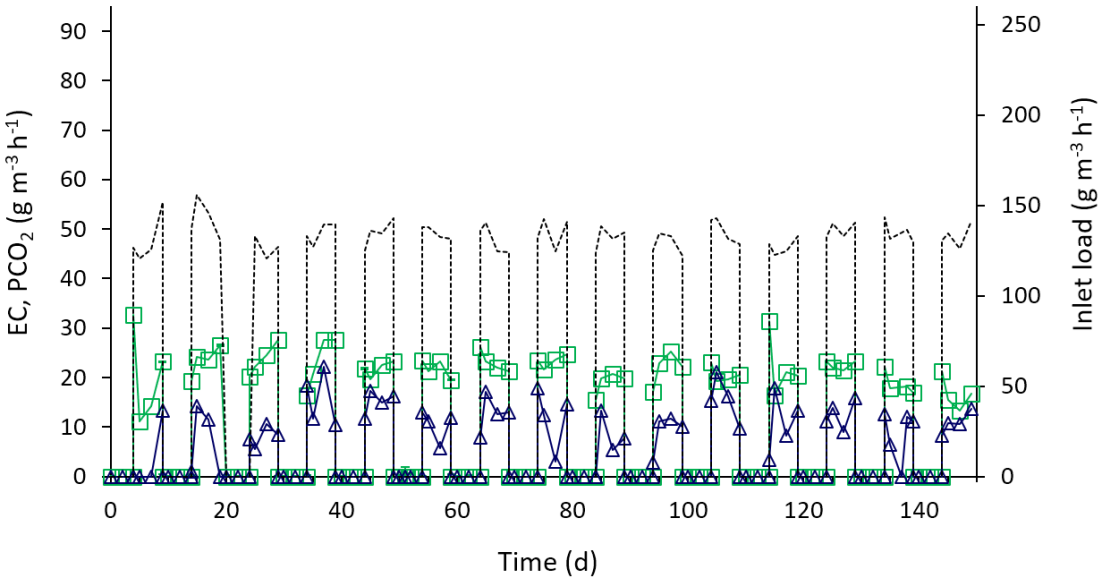
EC, PCO2 (g m-3 h-1)
Inlet load (g m-3 h-1)
Time (d)
0
10
20
30
40
50
60
70
80
90
0
50
100
150
200
250
0
20
40
60
80
100
120
140

c)

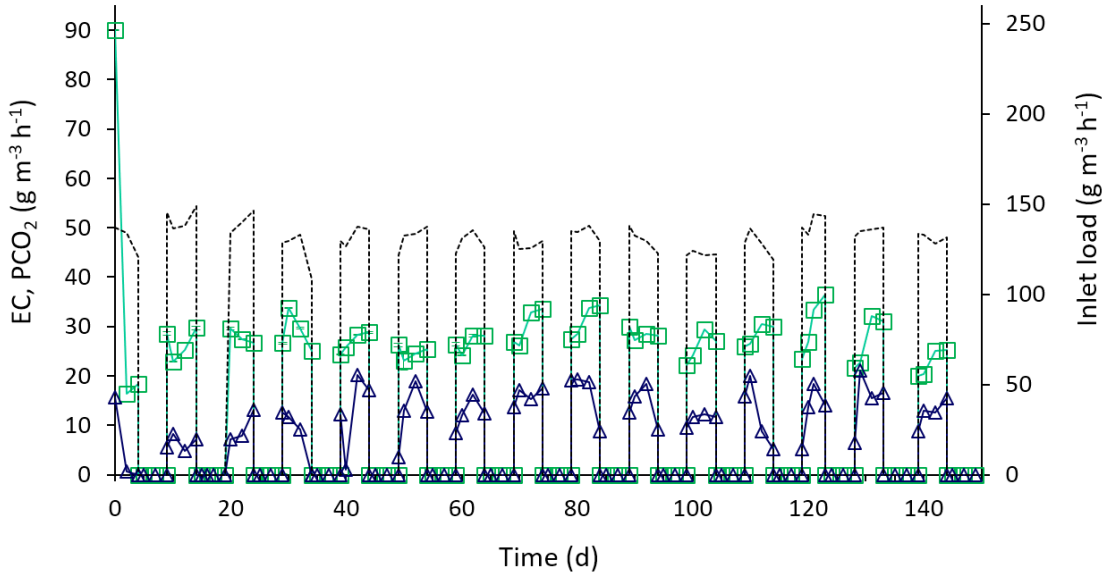
EC, PCO2 (g m-3 h-1)
Inlet load (g m-3 h-1)
Time (d)
0
10
20
30
40
50
60
70
80
90
0
50
100
150
200
250
0
20
40
60
80
100
120
140

Figure 4.

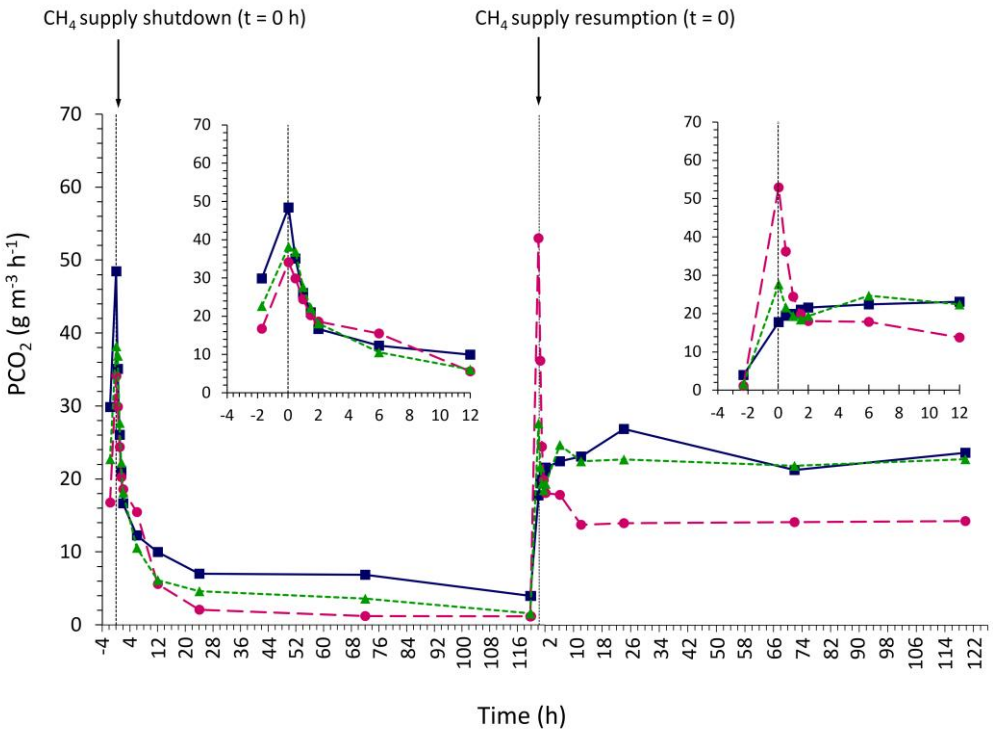
CH4 supply shutdown (t = 0 h)
CH4 supply resumption (t = 0)
PCO2 (g m-3 h-1)
Time (h)

Figure 5.

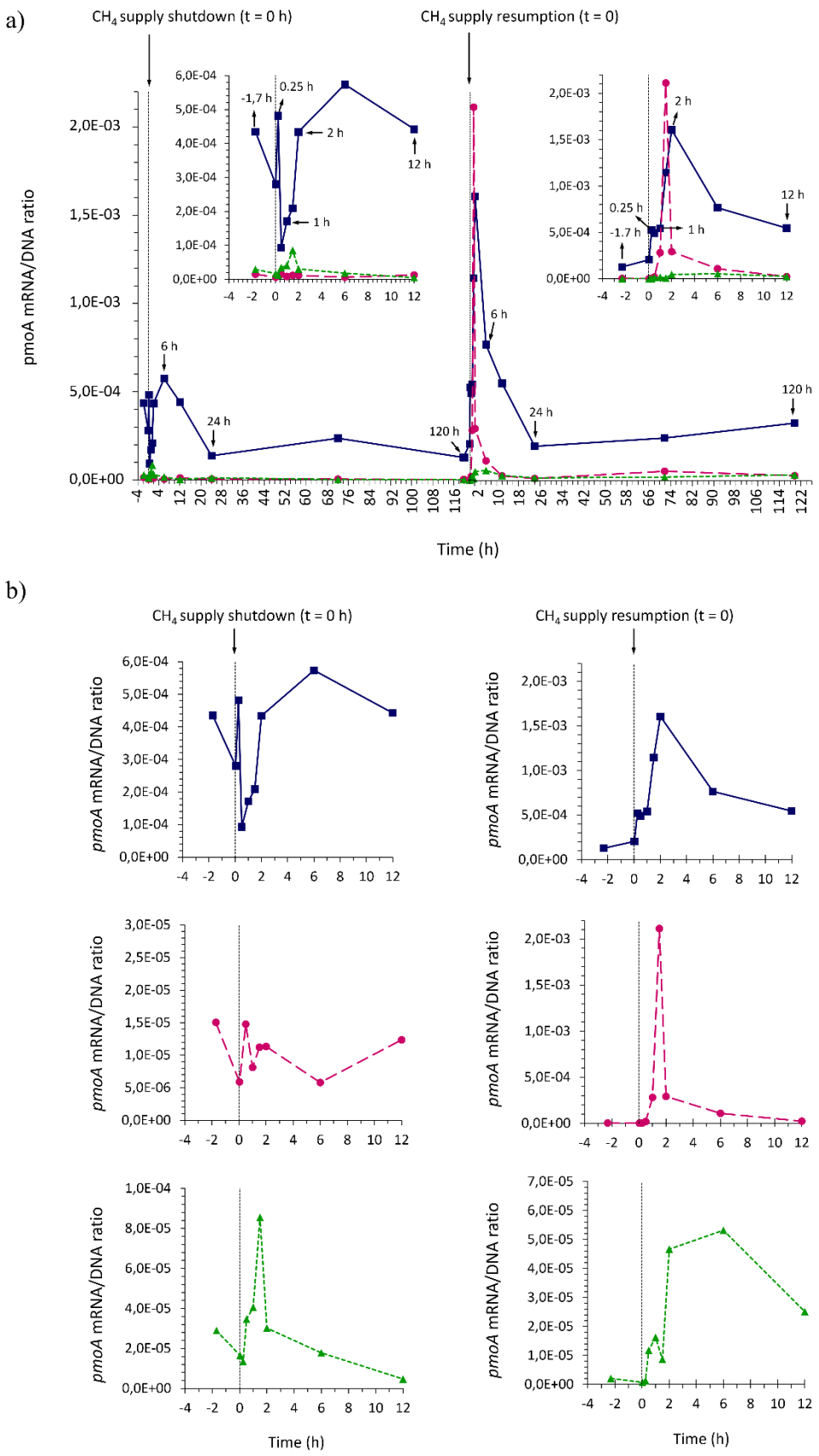
a)
CH4 supply shutdown (t = 0 h)
CH4 supply resumption (t = 0)
pmoA mRNA/DNA ratio
Time (h)
-1,7 h
0.25 h
2 h
12 h
1 h
6 h
24 h
120 h
b)
CH4 supply shutdown (t = 0 h)
CH4 supply resumption (t = 0)
pmoA mRNA/DNA ratio
Time (h)

Figure 6.

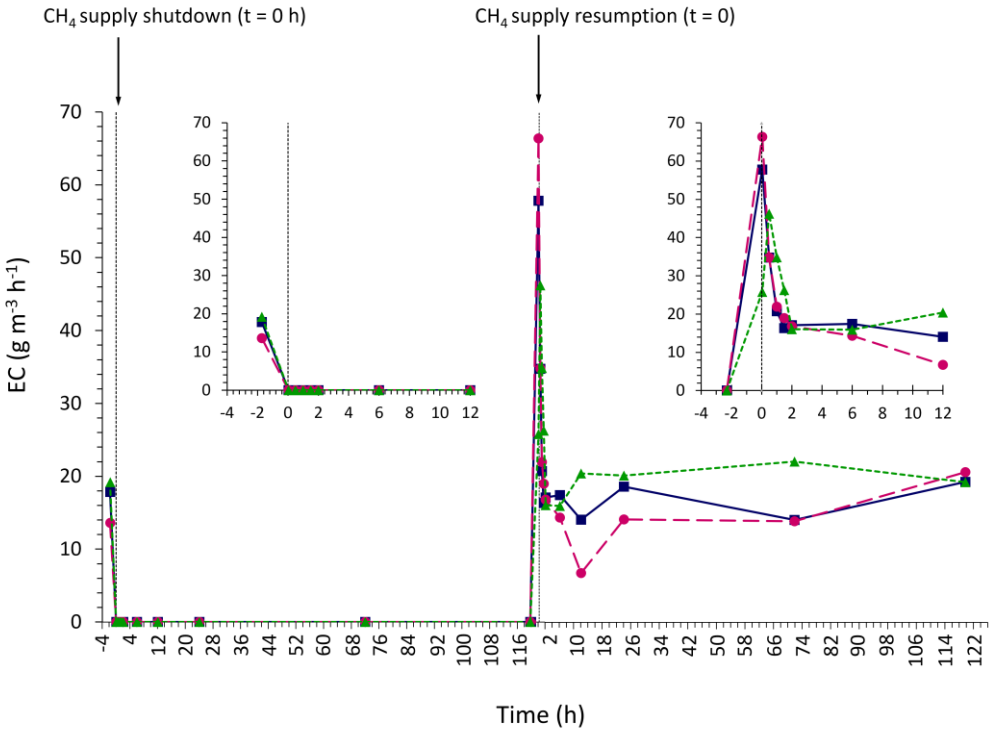
CH4 supply shutdown (t = 0 h)
CH4 supply resumption (t = 0)
EC (g m-3 h-1)
Time (h)

Table 1. mRNA / DNA ratios (copy mg VSS^{-1}) obtained by qPCR during the robustness analysis of the three STRs.

Time (h)	*pmoA* mRNA /DNA ratio (copy mg VSS^{-1})		
	STR 1	**STR 2**	**STR 3**
Famine			
-1.7	4.3×10^{-4} (3.4×10^{-5})	1.5×10^{-5} (2.2×10^{-6})	2.9×10^{-5} (5.0×10^{-6})
0.03	2.8×10^{-4} (3.4×10^{-5})	5.9×10^{-6} (4.4×10^{-7})	1.7×10^{-5} (1.5×10^{-6})
0.25	4.8×10^{-4} (5.9×10^{-5})	-	1.3×10^{-5} (3.9×10^{-7})
0.5	9.3×10^{-5} (1.4×10^{-5})	1.5×10^{-5} (1.2×10^{-5})	3.5×10^{-5} (3.5×10^{-6})
1	1.7×10^{-4} (1.2×10^{-5})	8.1×10^{-6} (9.5×10^{-7})	4.0×10^{-5} (5.1×10^{-6})
1.5	2.1×10^{-4} (3.3×10^{-5})	1.1×10^{-5} (1.5×10^{-6})	8.5×10^{-5} (4.6×10^{-6})
2	4.3×10^{-4} (7.1×10^{-5})	1.1×10^{-5} (2.4×10^{-6})	3.0×10^{-5} (4.1×10^{-6})
6	5.7×10^{-4} (9.8×10^{-5})	5.8×10^{-6} (5.2×10^{-7})	1.8×10^{-5} (1.3×10^{-6})
12	4.4×10^{-4} (7.4×10^{-5})	1.2×10^{-5} (1.6×10^{-6})	4.8×10^{-6} (7.9×10^{-7})
24	1.4×10^{-4} (2.0×10^{-5})	5.8×10^{-6} (3.5×10^{-7})	1.3×10^{-5} (4.9×10^{-7})
72	2.4×10^{-4} (3.9×10^{-5})	5.5×10^{-6} (4.4×10^{-7})	3.2×10^{-6} (5.0×10^{-7})
120 = -2.3	1.3×10^{-4} (1.7×10^{-5})	2.9×10^{-6} (2.2×10^{-7})	2.0×10^{-6} (6.0×10^{-7})
Feast			
0.03	2.0×10^{-4} (1.6×10^{-5})	4.4×10^{-7} (8.8×10^{-8})	6.9×10^{-7} (1.5×10^{-7})
0.25	5.2×10^{-4} (3.0×10^{-5})	4.2×10^{-6} (2.5×10^{-7})	1.3×10^{-6} (2.5×10^{-7})
0.5	4.9×10^{-4} (7.9×10^{-5})	1.8×10^{-5} (3.3×10^{-6})	1.2×10^{-5} (1.4×10^{-6})
1	5.4×10^{-4} (1.1×10^{-4})	2.8×10^{-4} (2.2×10^{-5})	1.6×10^{-5} (4.3×10^{-7})
1.5	1.1×10^{-3} (1.3×10^{-4})	2.1×10^{-3} (2.5×10^{-4})	8.7×10^{-6} (1.8×10^{-6})
2	1.6×10^{-3} (9.1×10^{-5})	2.9×10^{-4} (2.4×10^{-5})	4.7×10^{-5} (8.8×10^{-6})
6	7.7×10^{-4} (6.6×10^{-5})	1.1×10^{-4} (1.3×10^{-5})	5.3×10^{-5} (4.4×10^{-6})
12	5.5×10^{-4} (6.1×10^{-5})	2.3×10^{-5} (2.4×10^{-6})	2.5×10^{-5} (2.9×10^{-6})
24	1.9×10^{-4} (1.7×10^{-5})	8.1×10^{-6} (1.2×10^{-6})	1.2×10^{-5} (2.5×10^{-6})
72	2.4×10^{-4} (1.9×10^{-5})	4.9×10^{-5} (8.9×10^{-6})	1.6×10^{-5} (1.3×10^{-6})
120	3.2×10^{-4} (2.7×10^{-5})	2.4×10^{-5} (5.1×10^{-6})	2.9×10^{-5} (5.0×10^{-6})

Supplementary Material Rodriguez et al

Data Statement

Click here to download Data Statement: dataprofile.xml